Heteroatom Chemistry
Volume 13, Number 6, 2002

Designer Haem Proteins: What Can We Learn from Protein Engineering?

Emma Lloyd Raven

Department of Chemistry, University of Leicester, University Road, Leicester, LE1 7RH, England, UK

Received 29 March 2002

ABSTRACT: *Iron protoporphyrin(IX) is one of the most versatile and widespread pieces of catalytic machinery known in biology and is a key component of a multitude of proteins and enzymes. One of most challenging questions in this area has been to identify and understand the relationships that exist between different classes of haem proteins and to use protein engineering methods to rationalize the mechanisms by which the protein structure controls the specific chemical reactivity of the haem group. The application of this approach to the haem enzyme ascorbate peroxidase and the haem protein leghaemoglobin is discussed.* © 2002 Wiley Periodicals, Inc. Heteroatom Chem 13:501–505, 2002; Published online in Wiley InterScience (www.interscience.wiley.com). DOI 10.1002/hc.10094

INTRODUCTION

Iron protoporphyrin(IX) (Fig. 1) is one of the most versatile and widespread pieces of catalytic machinery known in biology and is a key component of a multitude of proteins and enzymes, including oxygen carriers, electron transfer proteins, peroxidases, and monooxygenases. One of most challenging questions in this area has been to identify and understand the relationships that exist between different classes of haem proteins, that is, to rationalize the mechanisms by which the protein *structure* controls the specific chemical *reactivity* of the haem group [1,2].

A particularly powerful experimental method that has been used in the study of haem structure/function relationships is site-directed mutagenesis. In this approach, key amino acid substitutions are engineered into the protein architecture and the functional consequences of these changes are established later using a range of techniques. In many cases, the protein engineering approach is made more powerful by the availability of structural information for the protein of interest and, in this way, structural information can provide the conceptual platform upon which targeted amino substitutions are visualized.

In this paper, we describe the application of this approach to the study of two recombinant haem proteins: pea cytosolic ascorbate peroxidase (rAPX) and soybean leghaemoglobin *a* (rLb).

ASCORBATE PEROXIDASE

Ascorbate peroxidase (APX) is a member of the haem peroxidase family of enzymes and catalyzes the ascorbate-dependent reduction of potentially damaging hydrogen peroxide in plants and algae, Eq. (1).

$$2\ \text{ascorbate} + H_2O_2 \rightarrow 2\ \text{monodehydroascorbate} + 2H_2O \quad (1)$$

Ascorbate-dependent peroxidase activity was first reported in 1979 [3,4] and in 1991 the first crystal structure for an APX enzyme was published [5]. This information, together with the availability of a recombinant expression system for the pea cytosolic enzyme [6], served as a catalyst for the publication of new functional and spectroscopic data and has

Correspondence to: Emma Raven; e-mail: emma.raven@le.ac.uk.
Contract grant sponsor: BBSRC, EPSRC, and The Royal Society.
© 2002 Wiley Periodicals, Inc.

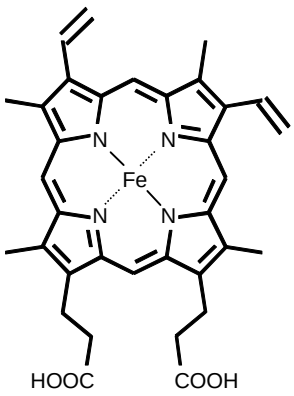

FIGURE 1 The structure of iron protoporphyrin(IX).

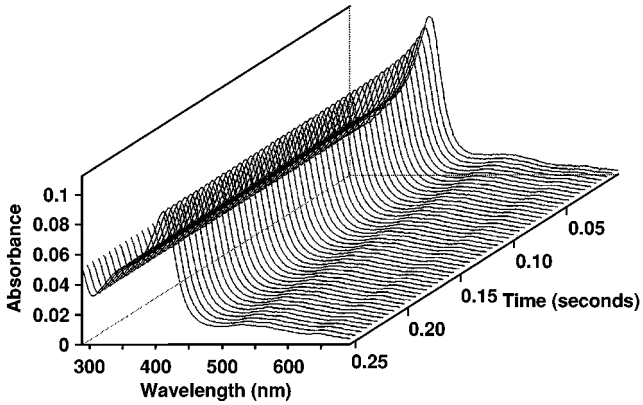

FIGURE 2 Time dependent spectroscopic changes for the formation of Compound **I** for rAPX ([rAPX]= 1 μM, $[H_2O_2]$ = 1 μM, 5°C, sodium phosphate, pH 7.0, $\mu = 0.10$ M). A total of 100 spectra were collected and every second spectrum is shown.

meant that these data could be sensibly rationalized at the molecular level. We have examined several aspects of the rAPX enzyme by using protein-engineering methodology.

Catalytic Mechanism

The APX enzyme operates through a classical peroxidase mechanism in which the ferric enzyme is oxidized by two electrons to a so-called Compound **I** intermediate with concomitant release of 1 molecule of water, followed by two successive single electron reductions of the intermediate by ascorbate (HS) to regenerate ferric enzyme, Eq. (2)–(4).

$$\text{APX} + \text{H}_2\text{O}_2 \xrightarrow{k_1} \text{Compound } \mathbf{I} + \text{H}_2\text{O} \quad (2)$$

$$\text{Compound } \mathbf{I} + \text{HS} \xrightarrow{k_2} \text{Compound } \mathbf{II} + \text{S}^{\cdot} \quad (3)$$

$$\text{Compound } \mathbf{II} + \text{HS} \xrightarrow{k_3} \text{APX} + \text{S}^{\cdot} + \text{H}_2\text{O} \quad (4)$$

Although steady state kinetic analyses have been a fairly prominent feature of most of the early literature on APX (reviewed in [7]), presteady-state kinetic data has been very much more limited [8–13].

Formation of Compound **I** for wild-type rAPX [14] (Fig. 2) was rapid and linear dependencies of the observed rate constant on peroxide concentration are observed. A second-order rate constant of $k_1 = 6.1 \pm 10^7\ \text{M}^{-1}\,\text{s}^{-1}$ is derived. The enzyme was also reactive towards other peroxides, microscopic rate constants for reaction of APX with various peroxides are given in Table 1.

When the distal histidine 42 residue (Fig. 3) was replaced with an alanine (H42A variant [14]) or glutamic acid (H42E variant [14]) residue, the rate of Compound **I** formation was dramatically reduced [14]. In this case, a hyperbolic dependence of observed rate constant on peroxide concentration is observed, consistent with a mechanism involving formation of an intermediate (X), Eq. (5) and (6)

$$\text{E} + \text{H}_2\text{O}_2 \overset{K_a}{\longleftrightarrow} \text{X} \quad (5)$$

$$\text{X} \xrightarrow{k'_1} \text{Compound } \mathbf{I} + \text{H}_2\text{O} \quad (6)$$

(E = H42A or H42E). This mechanism predicts a hyperbolic dependence and a fit of the data to Eq. (7)

$$k_{1,\text{obs}} = \frac{k'_1}{1 + K_d/[\text{H}_2\text{O}_2]} \quad (7)$$

yields values for k'_1, the limiting rate constant, and K_d of $(4.3 \pm 0.2)\ \text{s}^{-1}$ and (30 ± 2.0) mM, respectively (H42A) and $(28 \pm 0.7)\ \text{s}^{-1}$ and (0.09 ± 0.01) mM, respectively (H42E). This mechanism suggests the accumulation of an intermediate, the conversion of which to product is rate-limiting at high peroxide concentrations. Intermediate spectra obtained from a spectrally deconvoluted model are shown for H42A in Fig. 4. The spectrum of the intermediate has features at 401 nm, 522 nm, and 643 nm, which we assign as arising from a transient [enzyme-H_2O_2] intermediate. Detection of this species, the first time for an APX, is only possible in the H42A variant as a result of the dramatically reduction in rate constant for Compound **I** formation.

TABLE 1 Second-Order Rate Constants for the Formation of Compound **I** upon Reaction with Various Peroxides

Peroxide	$k_1\ (M^{-1}\,s^{-1})$
H_2O_2	$6.1 \pm 0.1 \times 10^7$
Peracetic acid	$4.9 \pm 0.1 \times 10^7$
m-Chloroperoxybenzoic acid	$1.1 \pm 0.2 \times 10^7$

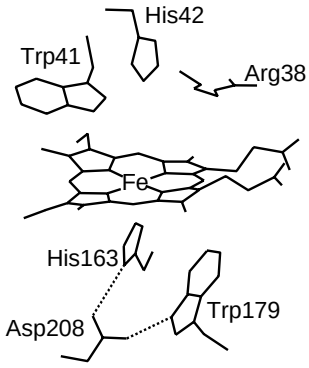

FIGURE 3 The active site of ascorbate peroxidase [5].

Examination of the hydrogen ion dependences of the observed rate constants for Compound **I** formation for rAPX, H42A, and H42E enzymes is also very informative and identifies the distal histidine 42 residue as being the catalytic acid-base residue in the mechanism, Scheme 1. pH-Dependent profiles are observed for rAPX ($pK_a = 4.9 \pm 0.1$) and H42E (6.7 ± 0.2), but a pH-independent profile is observed for H42A.

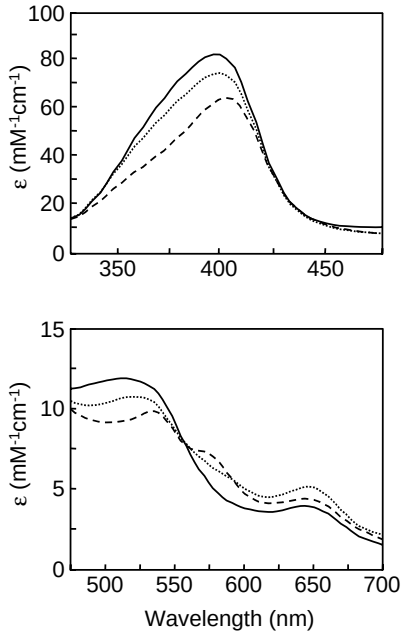

FIGURE 4 Photodiode array spectra (sodium phosphate, pH 7.0, $\mu = 0.10$ M, 5.0°C) for the reaction between H42A (1 μM) and H_2O_2 (35 mM). Experimental data were fitted to an A → B → C model, using Prokin Software. Deconvoluted spectra from this analysis are shown in the Soret (top) and visible (bottom) regions. The solid line is ferric H42A; the dotted and dashed lines show spectra derived from the model, and represent the spectra of the proposed [H42A-H_2O_2] complex and Compound **I**, respectively.

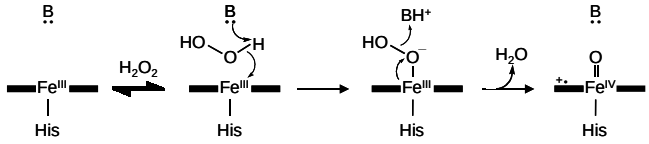

SCHEME 1 A proposed mechanism for formation of Compound **I**. The mechanism depicts the neutral peroxide-bound intermediate (X, see text). The distal histidine 42 residue is identified as the acid-base catalysts (B) from pH-dependent studies (see text).

Substrate Oxidation

We have proposed a structural model for the enzyme–substrate interaction in rAPX [16]. Reduction of Compound **I** by ascorbate is fast ($k_2 = 2.7 \pm 0.1 \times 10^7$ M^{-1} s^{-1}); reduction of Compound **II** is rate-limiting and shows saturation kinetics, with a limiting rate constant $k'_3 = (56 \pm 5)$ s^{-1} and $K_d = (307 \pm 44)$ μM, see Eq. (7).

In addition to oxidation of ascorbate, APX is also capable of oxidation of other (nonphysiological) aromatic substrates [17], e.g. *p*-cresol (**I**, Scheme 2). Kinetic parameters in this case are $k_2 = 5.4 \pm 0.1 \times 10^5$ M^{-1} s^{-1}, $k'_3 = (18.5 \pm 0.7)$ s^{-1}, and $K_d = 1.54 \pm 0.12 \times 10^{-3}$ M. HPLC, GC-MS, and NMR analyses are consistent with the formation of 2,2′-dihydroxy-5,5′-dimethylbiphenyl (**II**, Scheme 2) and 4a,9b-dihydro-8,9b-dimethyl-3(4H)-dibenzofuranone (Pummerer's ketone **III**, Scheme 2) as the major products.

Enantioselective sulphoxidation activity has also been engineered into the rAPX molecule [18]. This is of interest in relation to the haem-containing cytochrome P450 class of enzymes, which are not only able to catalyze the insertion of 1 mol oxygen into substrate—a reaction that peroxidases, with a few exceptions, are unable to support—but also to achieve this in a enantioselective manner. The molecular basis for these differences in reactivities is not completely understood but is likely to partly derive from variations in the axial ligation to the haem and the access of the substrate to the oxidized ferryl species [1,2]. Our preliminary examination of the crystal structure indicated that the distal

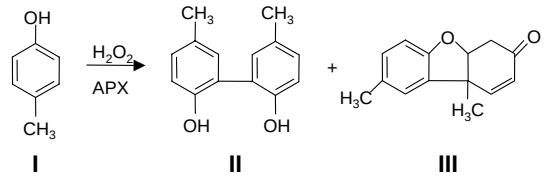

SCHEME 2 Products of the rAPX-catalysed oxidation of *p*-cresol (**I**) by hydrogen peroxide. The major products are 2,2′-dihydroxy-5,5′-dimethylbiphenyl (**II**), and Pummerer's ketone (**III**).

tryptophan residue at position 41 in rAPX (Fig. 3) may partially hinder access of substrate to the haem and may control the enantiomeric ratios of products. Hence, the oxidation of *p*-chlorophenyl methyl sulphide and *p*-nitrophenyl methyl sulphide by rAPX and a W41A site-directed variant has been examined (Scheme 3). For rAPX, racemic mixtures of *R*- and *S*-sulphoxides were obtained for both sulphides (R/S = 49:51 for *p*-chlorophenyl methyl sulphide and R/S = 48:52 for *p*-nitrophenyl methyl sulphide). The W41A variant shows enhancements in enantioselectivity for both sulphides (R/S = 65:35 for *p*-chlorophenyl methyl sulphide and R/S = 85:15 for *p*-nitrophenyl methyl sulphide). Direct oxygen atom transfer from the ferryl haem to the substrate was confirmed by labelling experiments with $H_2{}^{18}O_2$. Structure-based modeling techniques have indicated that reorientation of the side chain of Arg38, such that access to the haem is much less restricted, is influential in controlling the stereoselectivity for both rAPX and W41A, Fig. 5. A fully quantitative rationalization of the enantioselectivity was only possible when the side chain of Arg38 was reoriented, Fig. 5.

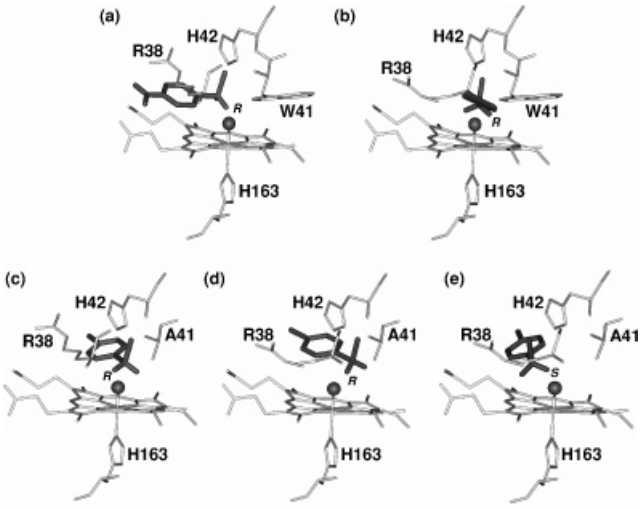

FIGURE 5 The orientation of *p*-nitrophenyl methyl sulphide (dark grey) binding at the active site of rAPX. (a): Arg38 orientation as in the crystal structure [5] with the pro-*R* lone pair close to the ferryl oxygen; an R/S ratio of 100:0 is predicted. (b): Arg38 orientation modified with the pro-*R* and pro-*S* lone pairs close to the ferryl oxygen; an R/S ratio of 53:47 is predicted close to the experimentally determined value of 48:52. The orientation of *p*-chlorophenyl methyl sulphide (dark grey) docked into the active site of W41A. (c): Arg38 orientation as in the crystal structure [5]: the pro-*R* lone pair close to the ferryl oxygen; an R/S ratio of 100:0 is predicted. (d and e): Arg 38 orientation modified with the pro-*R* lone pair close to the ferryl oxygen and a minority population of the pro-*S* lone pair close to the ferryl oxygen; an R/S ratio of 63:37 is predicted close to the experimentally determined value of 65:35.

Leghaemoglobin

Leghaemoglobin is a small haem-containing protein, which is found in the root nodules of leguminous plants and which regulates the supply of oxygen in nitrogen-fixing bacteria [19–21]. A crystal structure for the leghemoglobin *a* from soybean is shown in Fig. 6 [22,23]. We have reported [24] the generation of a synthetic gene for soybean Lb*a* and have established that the recombinant protein derived from expression of this gene in *Escherishcia coli* is an authentic duplicate of the wild-type soybean Lb*a*. We have used this expression system to probe various functional aspects of the molecule. For example, a strategic assessment [25] of the contributions of two active site hydrogen bonds in the binding of nicotinate—a physiological ligand—to rLb has been carried out by mutagenic replacement of the hydrogen-bonding residues (H61A and Y30A variants, Fig. 6). Dissociation constants, K_d (pH 5.5, $\mu = 0.10$ M, $(25 \pm 0.1)^\circ$C), for binding of nicotinate to ferric rLb, H61A, and Y30A were (1.4 ± 0.3) μM, (19 ± 1) μM, and (11 ± 1) μM respectively, and provide the first quantitative assessment of the role of individual hydrogen bonds in the binding process. pH-Dependent binding experiments for the H61A variant identify the distal histidine residue as controlling the binding of nicotinate in the neutral to alkaline region.

Crystallographic studies [22,23] of soybean leghaemoglobin have revealed a larger, more accessible,

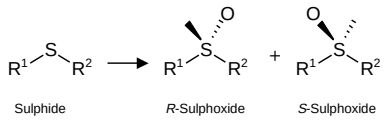

SCHEME 3 Products of the APX-catalyzed oxidation of Sulphides. R^1 is an aromatic group; R^2 is an alkyl group.

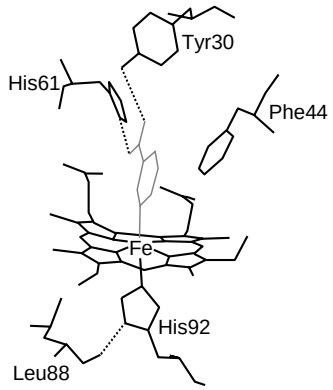

FIGURE 6 The active site of soybean leghaemoglobin *a*, showing the active site amino acids and the haem. Nicotinate (grey) is bound to the haem on the distal side.

and more flexible distal haem pocket than that is encountered in other mammalian globins. This conformational flexibility gives rise to a mobile switching histidine ligand (His61, Fig. 6), which, from spectroscopic studies [21,26] has been implicated in binding to the ferric haem species at low temperature to generate a low-spin, bis-histidine haem derivative. We have exploited this unique mobility of the leghaemoglobin molecule in the study of haem structure/function relationships by using it as an experimental framework for the examination of the effect of axial ligand substitutions by protein engineering. Hence, we have established that the incorporation of a nonligating amino acid essentially eliminates the low-spin haem species [27] and have shown that it is possible to incorporate new ligands into this flexible haem architecture by replacement of the switching histidine 61 ligand with other amino acids capable of haem ligation (H61Y and H61K variants).

ACKNOWLEDGMENTS

The author expresses her gratitude to the various students, postdoctoral assistants, and technicians who have contributed to this work including Deborah Jones, Daniel Turner, Latesh Lad, Adrian Hill, Neesha Patel, Martin Mewies, Katie Sharp, Ayhan Celik, and Kuldip Singh.

REFERENCES

[1] Dawson, J. H. Science 1988, 240, 433.
[2] Ortiz de Montellano, P. R. Acc Chem Res 1987, 20, 289.
[3] Groden, D.; Beck, E. Biochim Biophys Acta 1979, 546, 426.
[4] Kelly, G. J.; Latzko, E. Naturwissenschaften 1979, 66, 617.
[5] Patterson, W. R.; Poulos, T. L. Biochemistry 1995, 34, 4331.
[6] Patterson, W. R.; Poulos, T. L. J Biol Chem 1994, 269, 17020.
[7] Raven, E. L. In Subcellular Biochemistry: Enzyme Catalysed Electron and Radical Transfer; Holzenberg, A.; Scrutton, N. S. (Eds.); Kluwer/Plenum: London, 2000; p. 318.
[8] Pappa, H.; Patterson, W. R.; Poulos, T. L. J Biol Inorg Chem 1996, 1, 61.
[9] Marquez, L. A.; Quitoriano, M.; Zilinskas, B. A.; Dunford, H. B. FEBS Lett 1996, 389, 153.
[10] Kvaratskhelia, M.; Winkel, C.; Thorneley, R. N. F. Plant Physiol 1997, 114, 1237.
[11] Kvaratskhelia, M.; Winkel, C.; Naldrett, M. T.; Thorneley, R. N. F. J Plant Physiol 1999, 154, 273.
[12] Bursey, E. H.; Poulos, T. L. Biochemistry 2000, 39, 7374.
[13] Mandelman, D.; Jamal, J.; Poulos, T. L. Biochemistry 1998, 37, 17610.
[14] The recombinant wild type pea cytosolic enzyme is abbreviated as rAPX and has no mutations. The nomenclature for the site-directed variants is as follows: XYZ, where X is the amino acid found in the wild type protein, Y is the position in the sequence of this amino acid, and Z is the amino acid introduced by the mutation. Hence, replacement of histidine 42 by alanine is abbreviated to H42A and replacement of histidine 42 by glutamic acid is abbreviated as H42E.
[15] Lad, L.; Mewies, M.; Basran, J.; Scrutton, N. S.; Lloyd Raven, E. Eur J Biochem 2002, 269, 3182.
[16] Hill, A. P.; Modi, S.; Sutcliffe, M. J.; Turner, D. D.; Gilfoyle, D. J.; Smith, A. T.; Tam, B. M.; Lloyd, E. Eur J Biochem 1997, 248, 347.
[17] Celik, A.; Raven, E. L.; Cullis, P. M. Arch Biochem Biophys 2000, 373, 175.
[18] Celik, A.; Cullis, P. M.; Sutcliffe, M. J.; Sangar, R.; Raven, E. L. Eur J Biochem 2001, 268, 78.
[19] Davies, M. J.; Mathieu, C.; Puppo, A. Adv Inorg Chem 1999, 46, 495.
[20] Dilworth, M. J Meth Enzymol 1980, 69, 812.
[21] Appleby, C. A.; Blumberg, W. E.; Bradbury, J. H.; Fushman, W. H.; Peisach, J.; Wittenberg, B. A.; Wittenberg, J. B.; Wright, P. E. In Hemoglobin and Oxygen Binding; Ho, C. (Ed.); Elsevier: Amsterdam, 1982, p. 435.
[22] Ellis, P. J.; Appleby, C. A.; Guss, J. M.; Hunter, W. N.; Ollis, D. L.; Freeman, H. C. Acta Cryst D 1997, 53, 302.
[23] Ollis, D. L.; Appleby, C. A.; Colman, P. M.; Cutten, A. E.; Guss, J. M.; Venkatappa, M. P.; Freeman, H. C. Aust J Chem 1983, 36, 451.
[24] Jones, D. K.; Badii, R.; Rosell, F. I.; Lloyd, E. Biochem J 1998, 330, 983.
[25] Patel, N.; Jones, D. K.; Raven, E. L. Eur J Biochem 2000, 267, 2581.
[26] Sievers, G.; Gadsby, P. M. A.; Peterson, J.; Thomson, A. J Biochim Biophys Acta 1983, 742, 637.
[27] Patel, N.; Jones, D. K.; Cheesman, M. R.; Thomson, A. J.; Raven, E. L. Inorg Chim Acta 2002, 331, 303.